

Sintering and Electrical Properties of Lead-Free $\text{Na}_{0.5}\text{K}_{0.5}\text{NbO}_3$ Piezoelectric Ceramics

Ruzhong Zuo[†] and Jürgen Rödel*

Institute of Materials Science, University of Technology, D-64287 Darmstadt, Germany

Renzheng Chen and Longtu Li*

State Key Lab of New Ceramics and Fine Processing, Department of Materials Science and Engineering, Tsinghua University, Beijing, 100084, China

Lead-free $\text{Na}_{0.5}\text{K}_{0.5}\text{NbO}_3$ (NKN) piezoelectric ceramics were fairly well densified at a relatively low temperature under atmospheric conditions. A relative density of 96%–99% can be achieved by either using high-energy attrition milling or adding 1 mol% oxide additives. It is suggested that ultra-fine starting powders by active milling or oxygen vacancies and even liquid phases from B-site oxide additives mainly lead to improved sintering. Not only were dielectric properties influenced by oxide additives, such as the Curie temperature (T_c) and dielectric loss (D), but also the ferroelectricity was modified. A relatively large remanent polarization was produced, ranging from 16 $\mu\text{C}/\text{cm}^2$ for pure NKN to 23 $\mu\text{C}/\text{cm}^2$ for ZnO-added NKN samples. The following dielectric and piezoelectric properties were obtained: relative permittivity $\epsilon_{33}^T/\epsilon_0 = 570\text{--}650$, planar mode electromechanical coupling factor, $k_p = 32\%\text{--}44\%$, and piezoelectric strain constant, $d_{33} = 92\text{--}117$ pC/N.

I. Introduction

PIEZOELECTRIC ceramics and single crystals have been widely used as actuator, transducer, and sensor materials. Lead-containing materials, such as $\text{Pb}(\text{ZrTi})\text{O}_3$, $\text{Pb}(\text{Mg}_{1/3}\text{Nb}_{2/3})\text{O}_3\text{--PbTiO}_3$, and $\text{Pb}(\text{Zn}_{1/3}\text{Nb}_{2/3})\text{O}_3\text{--PbTiO}_3$ in either ceramic or crystal form, are currently applied in industry.^{1–4} It is believed that in these systems, a high piezoelectric response is related to the morphotropic phase boundary (MPB) between rhombohedral, tetragonal, or monoclinic phases.^{5–7} However, the toxicity of lead oxide and its high vapor pressure during processing have led to a demand for alternative lead-free piezoelectric materials that are environment friendly from the viewpoint of sustainable development.

Research on lead-free piezoelectric materials was mainly focused on the following material systems: tungsten bronze-type materials, bi-layer structured materials, and perovskite-type materials. In terms of large crystal anisotropy and problems with sintering,^{8–10} the piezoelectric ceramics and single crystals with perovskite structures have been receiving attention, which mainly involve alkali niobates, modified alkali bismuth titanates, and systems in which an MPB occurs. KNbO_3 is one of them because single crystals show an excellent piezoelectric performance and a relatively high Curie temperature.^{11,12} Moreover, the solid solution of ferroelectric KNbO_3 and antiferroelectric NaNbO_3 also displays a good piezoelectric response, particularly for the

morphotropic phase boundary composition $\text{Na}_{0.5}\text{K}_{0.5}\text{NbO}_3$ (NKN), with piezoelectric properties of $d_{33} = 80$ pC/N, $k_p = 36\text{--}40\%$, $Q_m = 130$, and $\epsilon_{33}^T/\epsilon_0 = 290$, when it was prepared by ordinary sintering.^{13,14} The piezoelectric properties of NKN were first reported by Cross in the crystal form.¹⁵ However, this composition is difficult to densify by an ordinary sintering technique, due to high volatilization of potassium at a high temperature. Hot pressing, hot isostatic pressing, or spark plasma sintering has been used to achieve high densities.^{14,16–18} But the cost is relatively high. Therefore, it is pertinent to further improve sintering of NKN ceramics under normal atmospheric conditions, although solid solutions of NKN with different end members, such as LiNbO_3 and SrTiO_3 , have been reported, showing good sinterability and piezoelectric properties.^{19–21}

In terms of possible low-temperature sintering processes, the following aspects are often considered: (1) pressure or electric field-assisted sintering,^{14,16–18} (2) reduction in initial particle size, due to the fact that the driving force for sintering is inversely proportional to the particle size, (3) addition of a small amount of glass phase, (4) addition of some sintering aids, for example, some oxides as impurities, or (5) introduction of lattice defects by the aliovalent atomic constitution or the adjustment of stoichiometry. The application of some glass phases usually tends to degrade the electrical properties to some extent. The application of defect chemistry in fabricating electroceramics appears well-known, based on the fact that both sintering and properties can be influenced, with respect to issues no. 4 and 5 mentioned above. The application of ultrafine powder has received considerable attention, and can be achieved in many ways, showing efficient sinterability. Pressure or electric field, incorporatively or separately, aids sintering in several cases; yet, the cost concerning equipment and sintering atmosphere is relatively high. By comparison, ordinary sintering in air is cost effective. In the past few years, some attempts have been made to promote sintering of NKN ceramics by either adding excess niobium or doping with a low amount of alkaline-earth elements.^{22,23} Low-melting point lead oxide was used to improve the sintering of NKN ceramics.^{24,25} In this work, this intention will be continued by investigating the effect of further oxides as sintering aids on the sinterability and the electrical performance of NKN ceramics. Additionally, high-energy attrition milling was applied after calcination to reduce the initial particle size. The effect of the milling process on the densification behavior of this material is also reported.

II. Experimental Procedure

The stoichiometric composition of $\text{Na}_{0.5}\text{K}_{0.5}\text{NbO}_3$ was made from the following starting materials: K_2CO_3 (>99.0%, Alfa Aesar, Karlsruhe, Germany), Na_2CO_3 (99.5%, Alfa Aesar), and Nb_2O_5 (99.9%, ChemPur, Karlsruhe, Germany). All of the starting materials were weighed according to the chemical formula and ball milled with a planetary mill in anhydrous ethanol

M. Kuwabara—contributing editor

Manuscript No. 20974. Received September 8, 2005; approved February 3, 2006.

Supported by the Deutsche Forschungsgemeinschaft (SFB 595).

*Member, American Ceramic Society.

[†]Author to whom correspondence should be addressed. e-mail: zuo@ceramics.tu-darmstadt.de

for 24 h. After drying, the mixed powder was calcined in an alumina crucible at 950°C for 3 h. The calcined powder was then attrition milled with cerium-stabilized zirconia balls 1–2 mm in diameter for 6–48 h using ethanol as the medium. In this step, 1 mol% dopant, such as Zn, Cd, Sn, Sc, W, Ce, or Y was added in its oxide form. The dried powder was compacted into disks of 10 mm diameter and 2 mm thickness under a uniaxial pressing in a stainless-steel die.

Sintering was carried out in air for 4 h by placing the samples on a platinum foil covered with an alumina crucible in order to prevent a reaction from occurring between the samples and the substrate, and to minimize the evaporation of potassium. The sintering temperature was in the range of 1020°C – 1130°C , at a heating rate of $300^\circ\text{C}/\text{h}$. The density of the sintered samples was measured by the Archimedes method. Powder X-ray diffraction (XRD, STOE, Darmstadt, Germany) patterns of crushed pellets were recorded in the 2θ range of 20° – 80° . The particle size distribution of the attrition-milled powders was analyzed by a particle sizer (BI-XDC, Brookhaven Instruments Corporation, Holtsville, NY). The microstructure of the sintered samples from natural surfaces or fracture surfaces was observed by means of high-resolution scanning electron microscopy (HR-SEM, Model No. XL 30 FEG, Philips Electronic Instruments, Mahwah, NJ).

The disks were ground and polished in order to obtain parallel surfaces. A silver paste (Gwent Electronic Materials Ltd., Pontypool, UK) was screen printed and then fired on both sides of the samples at 700°C for 30 min. Dielectric permittivity and loss were measured by an impedance analyzer (Mode: HP4284A, Hewlett-Packard Company, Palo Alto, CA) at different frequencies from 100 Hz to 1 MHz in the temperature range of 25°C – 500°C . Polarization and strain hysteresis loops were measured in a silicone oil bath by applying an electric field of triangular waveform at a frequency of 50 mHz. A poling treatment was conducted at 100°C in stirred silicone oil at 3 kV/mm for 30 min using a DC powder supply, and then the samples were cooled to room temperature by maintaining the electric field. The piezoelectric strain constant d_{33} was measured 24 h after poling by a quasi-static Berlincourt-meter (Model YE2730, SINOCERA, Shanghai, China). The planar electromechanical coupling factor k_p was obtained by a resonance-antiresonance method by an impedance analyzer (Mode: HP 4192A) on the basis of IEEE standards.²⁶

III. Results and Discussion

(1) Sintering of NKN Ceramics

Figure 1 shows the effect of the milling process on the sintering of NKN ceramic samples, which were sintered at different tem-

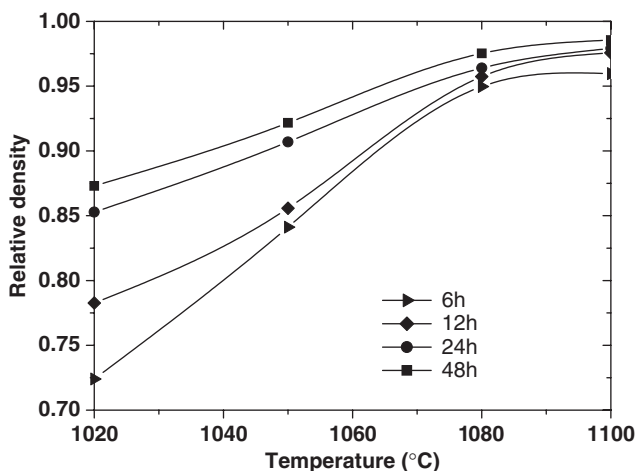


Fig. 1. Effect of attrition-milling process on sintering of Sandia National Laboratories ceramics.

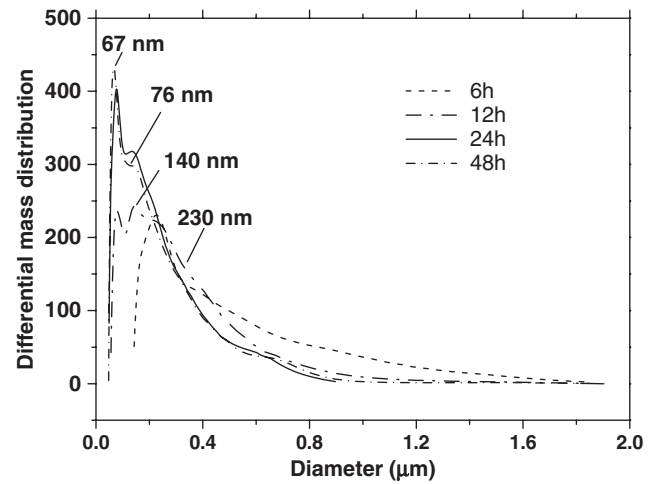


Fig. 2. Particle size distribution of the powders after being attrition milled for different times.

peratures for 4 h. The density of all samples increased with sintering temperature, and then slightly decreased when the temperature was above 1100°C , which was possibly due to the evaporation of potassium oxide at high temperature. All samples reached a density more than 96.5% of the theoretical density (TD, 4.51 g/cm^3)²⁷ at the sintering temperature of 1100°C , which was slightly lower than that of hot-pressed samples,¹⁶ but was rather difficult to reach applying conventional planetary ball milling. Moreover, with increasing attrition milling time, the densification improved clearly, as the reduced particle sizes provided larger driving forces for sintering. The particle size distribution of the powders after attrition milling is shown in Fig. 2. The initial particle size was sufficiently reduced to a mean particle size of $\sim 70\text{ nm}$. Conventional planetary milling was also used in this study to grind NKN powders, but the samples exhibited a highest density of only 94% TD. The samples made from 48 h attrition-milled powder reached a density of 98.5% TD at 1100°C . This indicates that a high-energy attrition-milling process is fairly efficient in improving the sintering of NKN ceramics under atmospheric pressure.

Additionally, various kinds of oxide sintering additives were used to improve the sintering of NKN. The effect of these oxides on densification is displayed in Fig. 3. Here all samples were sintered at different temperatures for 4 h. The densification was improved by adding 1 mol% oxides, such as ZnO, CdO, Sc_2O_3 , and SnO_2 ; however, the addition of oxides, like CeO_2 , Y_2O_3 , and WO_3 , severely inhibited sintering, as can be clearly seen from the curves in Fig. 3. Among them, the most pronounced

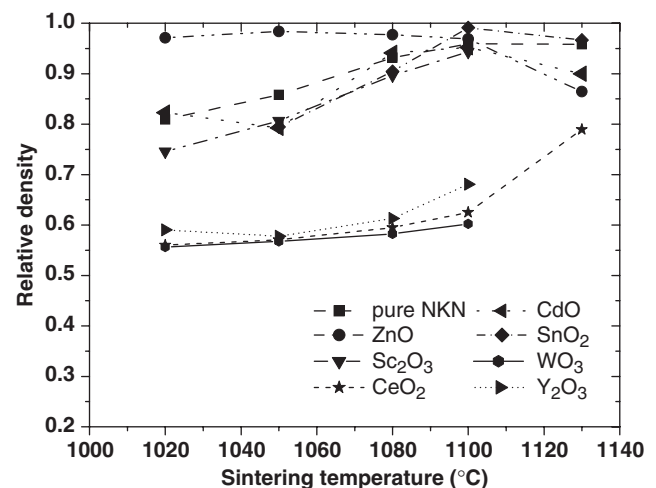


Fig. 3. Effect of 1 mol% oxide sintering additives on densification of $\text{Na}_{0.5}\text{K}_{0.5}\text{NbO}_3$ ceramics.

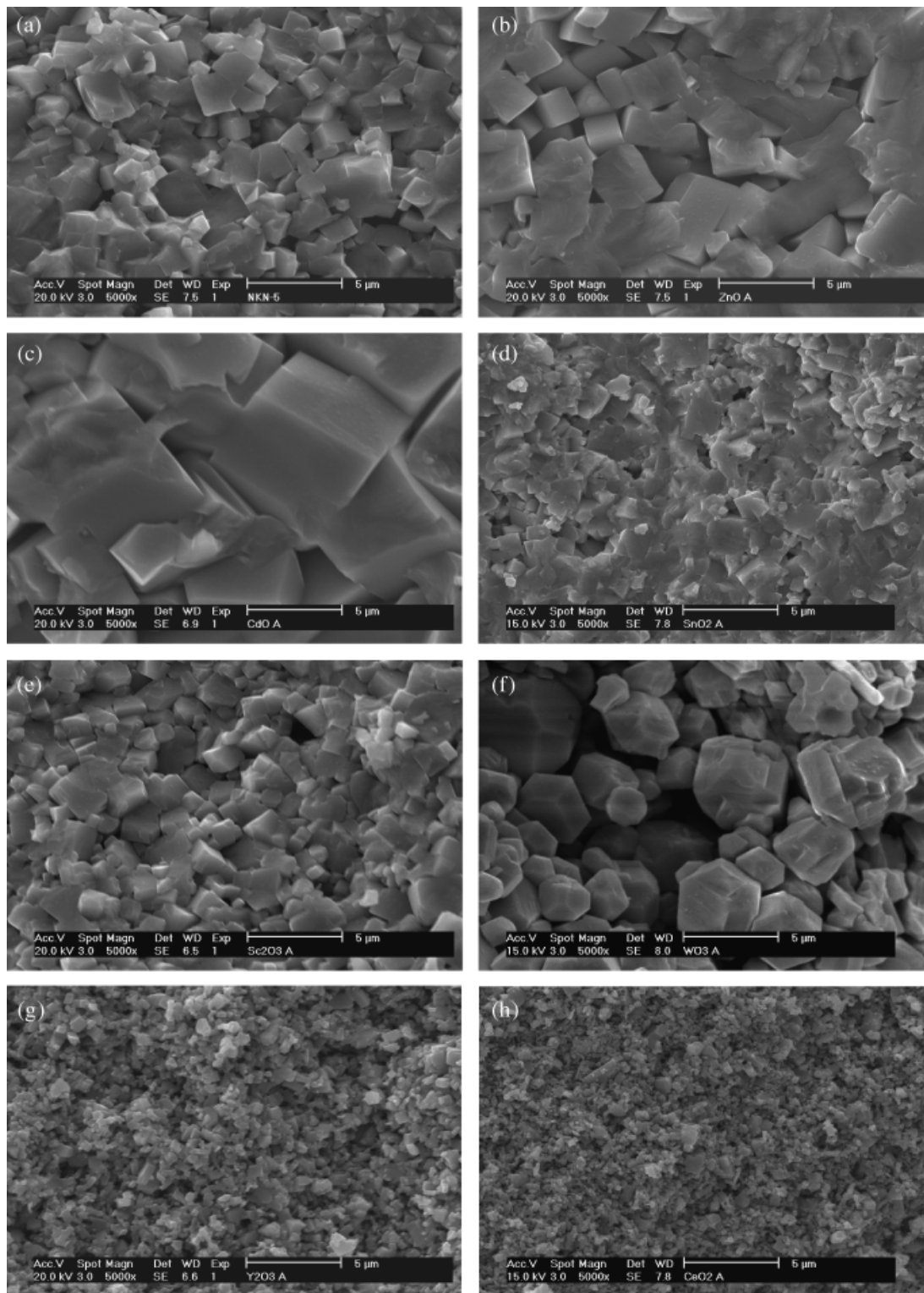


Fig. 4. Fracture morphology of $\text{Na}_{0.5}\text{K}_{0.5}\text{NbO}_3$ (NKN) samples with different oxide additives sintered at 1100°C for 4 h, (a) pure NKN, (b) ZnO, (c) CdO, (d) SnO_2 , (e) Sc_2O_3 , (f) WO_3 , (g) Y_2O_3 , and (h) CeO_2 .

improvement in NKN sintering was derived from the addition of ZnO and SnO_2 . A high density of up to 97.5% TD can be achieved at 1100°C by using 1 mol% ZnO as a sintering aid. Even at as low a temperature as 1000°C , the density of the sample is still as high as 96% of TD. In the case of ZnO addition, the sintering temperature for achieving good density can be lowered by 100°C . Pure NKN compositions from conventional planetary milling can hardly be sintered well in atmospheric pressure, as mentioned above. On the other hand, SnO_2 addition did not considerably decrease the sintering temperature, but it aided

densification significantly at a high temperature. Samples with SnO_2 addition showed more shrinkage at 1100°C than those without additives, exhibiting a density of 98.6% TD. The Sc_2O_3 addition did not improve the sintering considerably, as compared with pure NKN. Although CdO has a low melting point of 900°C , the sintering behavior of NKN ceramics did not improve considerably. The abnormal grain growth induced by the liquid phase of CdO (discussed later) could lead to a compromise in its contribution to sintering. Unfortunately, the thermal analysis results in this study did not show a difference between

pure and oxide-added NKN samples, probably because the amount of oxide additive was too low. The effect of each oxide additive on the sintering mechanism of NKN ceramics has not been clear so far.

The microstructure of NKN ceramics was also influenced by oxide sintering aids. The fracture morphology of NKN ceramics containing different kinds of oxide dopants is shown in Fig. 4. From these pictures, it is clear that these oxides have different effects on the microstructure. It is consistent with the density measurement, where oxides, like ZnO, SnO_2 , Sc_2O_3 , and CdO, changed the sintering of NKN ceramics to produce a dense microstructure. On the other hand, samples containing Y_2O_3 , WO_3 , or CeO_2 did not sinter considerably and were still rather porous. Additionally, the large difference in grain growth was clearly seen by using ZnO, SnO_2 , Sc_2O_3 , or CdO as sintering aids. The addition of CdO caused abnormal grain growth. Compared with pure NKN ceramics, the addition of ZnO promoted grain growth, but not as considerably as CdO. It is suggested that the rapid grain growth in the case of CdO is due to the low melting point (900°C) of CdO. For the same reason, abnormal grain growth inhibited sintering to some extent. Therefore, ZnO and SnO_2 can be considered good sintering additives for NKN ceramics from the viewpoint of microstructure and sintering.

(2) Dielectric Responses

Figure 5 shows the effect of 1 mol% oxide dopants on the dielectric properties of NKN samples at 1 MHz. Compared with pure NKN samples, the addition of oxide sintering additives reduces the Curie temperatures. Pure NKN ceramics have a Curie temperature of $\sim 418^\circ\text{C}$. Among the dopants, ZnO has the least effect on the Curie temperature. However, this finding

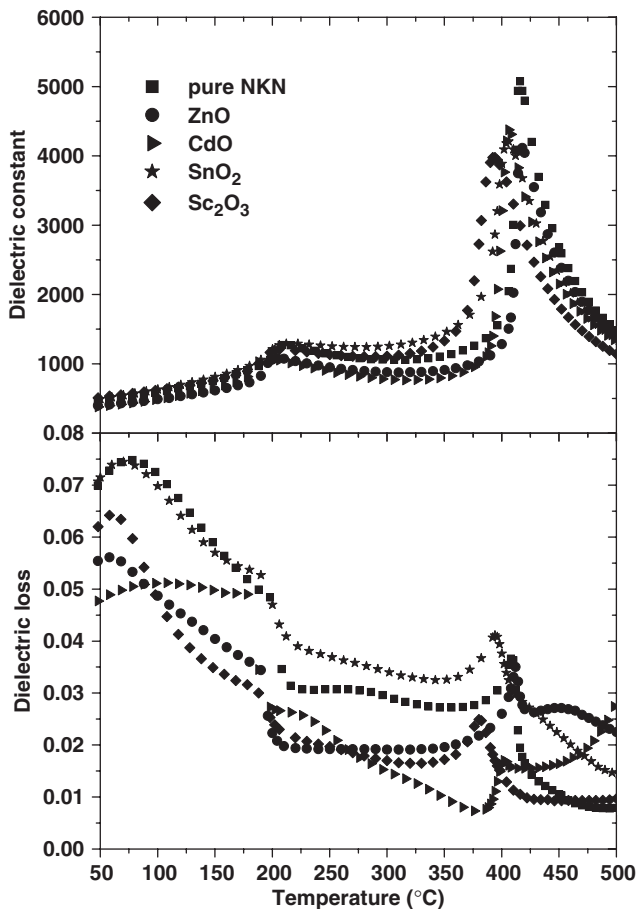


Fig. 5. Dielectric responses at 1 MHz as a function of measuring temperature for $\text{Na}_{0.5}\text{K}_{0.5}\text{NbO}_3$ ceramics with different sintering aids as indicated.

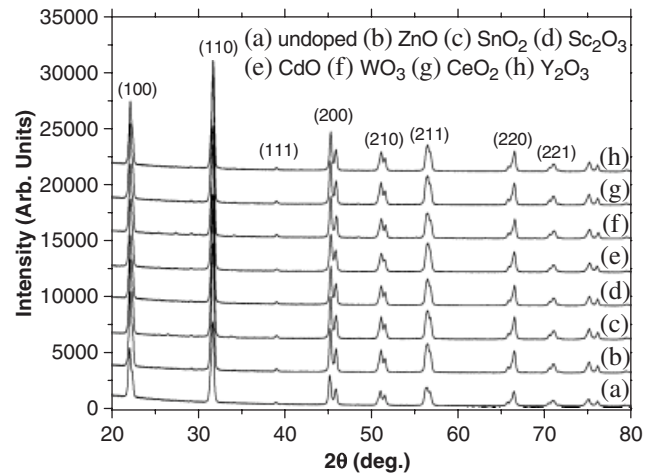


Fig. 6. X-ray diffraction pattern of $\text{Na}_{0.5}\text{K}_{0.5}\text{NbO}_3$ ceramics including various oxide sintering additives.

is different from that reported in the literature,²⁸ where the Curie temperature was decreased slightly by doping ZnO. The change in the Curie temperature further implies that the elements from these sintering aids entered the lattice of NKN ceramics. The addition of 1 mol% Sc_2O_3 decreased the Curie temperature by 24°C . In addition, the transition temperature from the orthorhombic to the tetragonal structure was also lowered by using sintering aids, which lies at 208°C for pure NKN. The dielectric loss was decreased to some extent by adding a small amount of

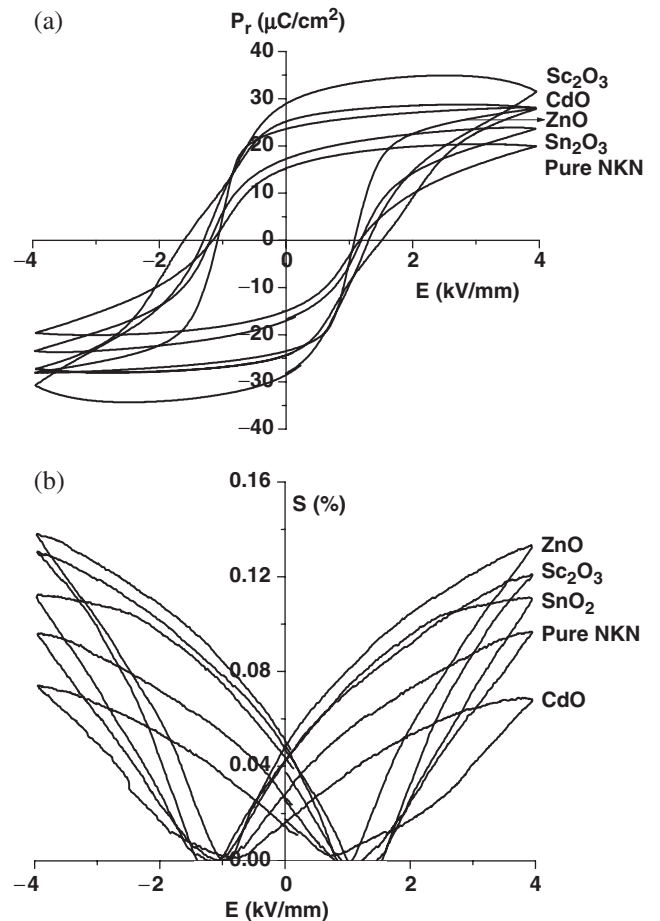


Fig. 7. Hysteresis loops of polarization (a) and strain (b) versus electric field at 50 mHz for two cycles.

Table I. Room-Temperature Dielectric Properties and Piezoelectric Responses of NKN Ceramics

Compositions	Pure NKN				NKN with sintering aids			
	ZnO	SnO ₂	Sc ₂ O ₃	CdO	ZnO	SnO ₂	Sc ₂ O ₃	CdO
Attrition-milling time (h)	6	12	24	48	6	6	6	6
Relative density (%)	96.0	97.6	98.0	98.4	97.0	98.0	94.2	95.3
Curie temperature (°C)	418	418	418	418	418	405	394	406
Dielectric permittivity at 25°C, 1 kHz	558	564	580	605	652	627	578	493
Loss tangent <i>D</i> (%) at 25°C, 1 kHz	3.47	3.52	3.92	4.36	3.33	4.56	5.01	4.04
Coupling factor <i>k_p</i> (%)	31	34	40	38	44	39	26	42
Piezoelectric charge constant <i>d₃₃</i> (pC/N)	92	99	107	102	117	108	100	107

NKN, Na_{0.5}K_{0.5}NbO₃.

oxide additives. The crystal structure of these compositions was verified by XRD, as shown in Fig. 6. It is evident that all compositions showed pure perovskite phases with orthorhombic symmetry. No secondary phases could be found due to the application of sintering aids. Also, the diffraction angles had not changed, indicating that the lattice constant had changed very little, probably because the level of adding oxide additives was low. As we can see, all oxide additives used in this study were considered to be B-site oxides in perovskite structures. Their cations own lower valences than five (Nb⁵⁺), except for W⁶⁺. Therefore, these additives can be viewed as acceptor dopants when they enter the lattice of NKN ceramics, and thereby, oxygen vacancies can be formed. Oxygen vacancies may improve sintering in some cases when oxides sinter in air. This fits the case of SnO₂-added NKN ceramics whose densification was enhanced only at a high temperature. For ZnO-added compositions, it could be expected that low-melting-point phases from a mixture of ZnO, K₂O, Na₂O, and Nb₂O₅ can be produced, which may aid low-temperature sintering of NKN ceramics. Therefore, measurement of dielectric properties may, to some extent, help in understanding the sintering mechanism of NKN ceramics, if oxide dopants are added.

(3) Hysteresis Loops of Polarization and Strain

Figure 7(a) shows the hysteresis loops of polarization versus electric field for NKN ceramics with different sintering aids measured at room temperature under an AC triangular waveform field of 50 mHz. The remanent polarization *P_r* and the coercive field *E_c* are 15.4 μC/cm² and 1.15 kV/mm, respectively, for pure NKN ceramics. These two values obviously changed with the addition of sintering aids, particularly the *P_r* value. The increase in *E_c* means that the materials become “harder,” which is consistent with the assumption that oxygen vacancies are formed by these oxide additives as acceptors. Exceptionally, ZnO had little effect on *E_c* of NKN ceramics. This further indicates that Zn ions do not enter the lattice to form oxygen vacancies. This observation is consistent with the fact that *T_c* had not clearly changed with addition of 1 mol% ZnO. The increase in remanent polarization and dielectric permittivity could be attributed to the enhanced density. The addition of 1 mol% ZnO increased *P_r* to 23.6 μC/cm². On the other hand, SnO₂, CdO, or Sc₂O₃ had an evident influence on the remanent polarization; at the same time, the coercive fields had also increased. The addition of 1 mol% Sc₂O₃ seemed to increase the *P_r* value by almost a factor of 2. However, the fact that the remanent polarization was larger than the saturated polarization at the maximum electric field applied indicated that the polarization was caused to some extent, by the leakage current or space charges.

From the corresponding strain versus field curves as shown in Fig. 7(b), it can be seen that a relatively small strain in CdO-added NKN samples was induced under the application of an AC field. This could be related to the heterogeneous microstructure. Another reason for this can be deduced from its polarization versus field curve, showing an irregular hysteresis loop where *E_c* had increased by 500 V/mm. In these curves in Fig. 7(b), the

maximum strain value *S_m* of 0.14% was produced under an AC electric field of 4 kV/mm for NKN ceramics containing 1 mol% ZnO, as compared with 0.09% for pure NKN samples.

(4) Electromechanical Properties

Piezoelectric properties of NKN samples manufactured by different attrition milling processing or by using a small amount of sintering additives are shown in Table I. For pure NKN samples, electromechanical coupling factor *k_p* varied in the range of 31%–40%, and piezoelectric charge constant *d₃₃* was in the range of 92–107 pC/N, which had improved obviously as compared with those published for pure NKN samples sintered under atmospheric conditions,^{19,20} as the density of the samples had increased up to 96.5%–98.5% TD with changing attrition milling time. As expected, the increased density also yielded a larger dielectric constant at room temperature. This could be one of the reasons for the increased *d₃₃* values, based on the fact that *d₃₃* is proportional to the dielectric constant.

For samples with oxide additives, the piezoelectric properties were even more improved. The *k_p* and *d₃₃* values for ZnO-added samples reached 44% and 117 pC/N, respectively. Therefore, these oxide additives not only improve the sintering behavior of NKN ceramics but also influence the electrical properties. Although the addition of most of these oxide additives lowers the Curie temperature somewhat, the enhanced density and improved piezoelectric properties demonstrate that they are beneficial for piezoelectric application of NKN ceramics.

IV. Conclusions

Sintering of lead-free Na_{0.5}K_{0.5}NbO₃ piezoelectric ceramics was improved by either using high-energy attrition milling or adding a small amount of oxide sintering additives. Dense homogeneous NKN samples were successfully fabricated with the density ranging from 96% to 99% under normal atmospheric sintering in air. Pure NKN samples showed *d₃₃* and *k_p* of 92–107 pC/N and 31%–40%, respectively. Oxide-doped NKN samples indicated not only an improved sintering behavior but also good electromechanical properties, particularly, *d₃₃* = 117, *k_p* = 44% for ZnO-aided samples and *d₃₃* = 108 pC/N, *k_p* = 39% in the case of SnO₂. NKN samples with oxide additives showed little or no deliquescence. The results in this study indicate that improved NKN ceramics can be good candidates for lead-free piezoelectric application.

References

1. B. Jaffe, W. R. Cook, and H. Jaffe, *Piezoelectric Ceramics*. Academic Press, New York, 1971.
2. Y. Lu, D. Y. Jeong, Z. Y. Cheng, Q. M. Zhang, H. S. Luo, Z. W. Yin, and D. Viehland, “Phase Transitional Behavior and Piezoelectric Properties of the Orthorhombic Phase of Pb(Mg_{1/3}Nb_{2/3})O₃-PbTiO₃ Single Crystals,” *Appl. Phys. Lett.*, **78** [20] 3109–11 (2001).
3. W. Ren, S. F. Liu, and B. K. Mukherjee, “Piezoelectric Properties and Phase Transitions of <001>-Oriented Pb(Zn_{1/3}Nb_{2/3})O₃-PbTiO₃ Single Crystals,” *Appl. Phys. Lett.*, **80** [17] 3174–6 (2002).

- ⁴S. E. Park and T. R. Shrout, "Ultrahigh Strain and Piezoelectric Behavior in Relaxor Based Ferroelectric Single Crystals," *J. Appl. Phys.*, **82** [4] 1804–11 (1997).
- ⁵R. Guo, L. E. Cross, S. E. Park, B. Noheda, D. E. Cox, and G. Shirane, "Origin of the High Piezoelectric Response in $\text{PbZr}_{1-x}\text{Ti}_x\text{O}_3$," *Phys. Rev. Lett.*, **84** [23] 5423–6 (2000).
- ⁶J. M. Kiat, Y. Uesu, B. Dkhil, M. Matsuda, C. Malibert, and G. Calvarin, "Monoclinic Structure of Unpoled Morphotropic High Piezoelectric PMN–PT and PZN–PT Compounds," *Phys. Rev. B*, **65**, 064106 (2002).
- ⁷A. K. Singh and D. Pandey, "Evidence for M_B and M_C Phases in the Morphotropic Phase Boundary Region of $(1-x)[\text{Pb}(\text{Mg}_{1/3}\text{Nb}_{2/3})\text{O}_3]_{1-x}\text{PbTiO}_3$: A Rietveld Study," *Phys. Rev. B*, **67**, 064102–1–12 (2003).
- ⁸M. Suzuki, H. Nagata, J. Ohara, H. Funakubo, and T. Takenaka, " $\text{Bi}_{3-x}\text{M}_x\text{TiTaO}_9$ ($M = \text{La}$ or Nd) Ceramics with High Mechanical Quality Factor Q_m ," *Jpn. J. Appl. Phys.*, **42** [9B] 6090–3 (2003).
- ⁹T. Sawada, A. Ando, Y. Sakabe, D. Damjanovic, and N. Setter, "Properties of the Elastic Anomaly in $\text{SrBi}_2\text{Nb}_2\text{O}_9$ -Based Ceramics," *Jpn. J. Appl. Phys.*, **42** [9B] 6094–8 (2003).
- ¹⁰R. J. Xie, Y. Akimune, R. Wang, N. Hirosaki, and T. Nishimura, "Dielectric and Piezoelectric Properties of Barium-Substituted $\text{Sr}_{1.9}\text{Ca}_{0.1}\text{NaNb}_5\text{O}_{15}$ Ceramics," *Jpn. J. Appl. Phys.*, **42** [12] 7404–9 (2003).
- ¹¹C. Zaldo, D.S. Gilled, R. W. Eason, J. Mendiola, and P. J. Chandler, "Growth of KNbO_3 Thin Films on MgO by Pulsed Laser Deposition," *Appl. Phys. Lett.*, **65** [4] 502–4 (1994).
- ¹²K. Yamanouchi, H. Odagawa, T. Kojima, and T. Matsumura, "Theoretical and Experimental Study of Superhigh Electromechanical Coupling Surface Acoustic Wave Propagation in KNbO_3 Single Crystal," *Electron. Lett.*, **33** [3] 193–4 (1997).
- ¹³L. Egerton and D. M. Dillon, "Piezoelectric and Dielectric Properties of Ceramics in the System Potassium Sodium Niobate," *J. Am. Ceram. Soc.*, **42** [9] 438–42 (1959).
- ¹⁴R. E. Jaeger and L. Egerton, "Hot Pressing of Potassium–Sodium Niobates," *J. Am. Ceram. Soc.*, **45** [5] 209–13 (1962).
- ¹⁵L. E. Cross, "Electric Double Hysteresis in $(\text{K}_x\text{Na}_{1-x})\text{NbO}_3$ Single Crystals," *Nature*, **181** [4603] 178–9 (1958).
- ¹⁶G. H. Haertling, "Properties of Hot-Pressed Alkali Niobate Ceramics," *J. Am. Ceram. Soc.*, **50** [6] 329–30 (1967).
- ¹⁷L. Egerton and C. A. Bieling, "Isostatically Hot-Pressed Sodium–Potassium Niobate Transducer Material for Ultrasonic Devices," *Ceram. Bull.*, **47**, 1151–6 (1968).
- ¹⁸R. Wang, R. Xie, T. Sekiya, and Y. Shimojo, "Fabrication and Characterization of Potassium–Sodium Niobate Piezoelectric Ceramics by Spark-Plasma-Sintering Method," *Mater. Res. Bull.*, **39**, 1709–15 (2004).
- ¹⁹Y. Guo, K. Kakimoto, and H. Ohsato, "Phase Transitional Behavior and Piezoelectric Properties of $\text{Na}_{0.5}\text{K}_{0.5}\text{NbO}_3$ – LiNbO_3 Ceramics," *Appl. Phys. Lett.*, **85** [18] 4121–3 (2004).
- ²⁰M. Kosec, V. Bobnar, M. Hrovat, J. Bernard, B. Malic, and J. Holc, "New Lead-Free Relaxor. Based on the $\text{K}_{0.5}\text{Na}_{0.5}\text{NbO}_3$ – SrTiO_3 Solid Solution," *J. Mater. Res.*, **19** [6] 1849–54 (2004).
- ²¹Y. Saito, H. Takao, T. Tani, T. Nonoyama, K. Takatori, T. Homma, T. Nagaya, and M. Nakamura, "Lead-Free Piezoceramics," *Nature*, **432**, 84–7 (2004).
- ²²Z. Ahn and W. A. Schulze, "Conventionally Sintered $(\text{Na}_{0.5}\text{K}_{0.5})\text{NbO}_3$ with Barium Additions," *J. Am. Ceram. Soc.*, **70** [1] C-18–21 (1987).
- ²³B. Malic, J. Bernard, J. Holc, D. Jenko, and M. Kosec, "Alkaline-Earth Doping in $(\text{K},\text{Na})\text{NbO}_3$ Based Piezoceramics," *J. Eur. Ceram. Soc.*, **25**, 2707–11 (2005).
- ²⁴S. Tashiro, H. Nagamatsu, and K. Nagata, "Sinterability and Piezoelectric Properties of KNbO_3 Ceramics After Substituting Pb and Na for K," *Jpn. J. Appl. Phys.*, **41** [11B, part 1] 7113–8 (2002).
- ²⁵S. Tashiro and K. Nagata, "Influence of Mixing Condition and Nonstoichiometry on Piezoelectric Properties of $(\text{KNaPb})\text{NbO}_3$ Ceramics," *Jpn. J. Appl. Phys.*, **43** [9B, part 1] 6711–5 (2004).
- ²⁶IEEE. *IEEE Standard on Piezoelectricity, ANSI/IEEE Standard No. 176-1987*. IEEE, New York.
- ²⁷M. Kosec and D. Kolar, "On Activated Sintering and Electrical Properties of NaKNbO_3 ," *Mater. Res. Bull.*, **10**, 335–40 (1975).
- ²⁸S. H. Park, C. W. Ahn, S. Nahm, and J. S. Song, "Microstructure and Piezoelectric Properties of ZnO-Added $(\text{Na}_{0.5}\text{K}_{0.5})\text{NbO}_3$ Ceramics," *Jpn. J. Appl. Phys.*, **43** [8B] L1072–4 (2004). □